

RealMind: Zero-Shot EEG-Based Visual Decoding and Captioning Using Multi-Modal Models

1st Dongyang Li*

Department of Biomedical Engineering
Southern University of Science and Technology
Shenzhen, China
lidy2023@mail.sustech.edu.cn

2nd Haoyang Qin*

Department of Biomedical Engineering
Southern University of Science and Technology
Shenzhen, China
12211832@mail.sustech.edu.cn

3rd Mingyang Wu

Department of Biomedical Engineering
Southern University of Science and Technology
Shenzhen, China
12312813@mail.sustech.edu.cn

4th Yuang Cao

Department of Biomedical Engineering
Southern University of Science and Technology
Shenzhen, China
12310901@mail.sustech.edu.cn

5th Chen Wei†

Department of Biomedical Engineering
Southern University of Science and Technology
Shenzhen, China
weic3@mail.sustech.edu.cn

6th Quanying Liu†

Department of Biomedical Engineering
Southern University of Science and Technology
Shenzhen, China
liuqy@sustech.edu.cn

Abstract—Despite significant progress in visual decoding with fMRI data, its high cost and low temporal resolution limit widespread applicability. To address these challenges, we introduce RealMind, a novel EEG-based visual decoding framework that leverages multi-modal models to efficiently interpret semantic information. By integrating semantic and geometric consistency learning, RealMind enhances feature alignment, leading to improved decoding performance. Our framework achieves a 56.73% Top-5 accuracy in a 200-way retrieval task and a 26.59% BLEU-1 score in a 200-way visual captioning task, representing the first successful attempt at zero-shot visual captioning using EEG data. RealMind provides a robust, adaptable, and cost-effective alternative to fMRI-based methods, offering scalable solutions for EEG-based visual decoding in practical applications.

Index Terms—Multi-modal models, EEG, visual decoding, representation learning, alignment.

I. INTRODUCTION

Multi-modal models represent an advanced class of machine learning frameworks designed to process and integrate diverse modalities of data [21], [23], [25]–[27]. These models are particularly noteworthy in the fields of neuroscience and machine learning due to their ability to simulate the human brain’s multisensory processing capabilities [22], [24], [28], [29]. Recent studies have demonstrated the efficacy of multi-modal models in achieving visual decoding with functional magnetic resonance imaging (fMRI) [5], [15], [16], [35]. However, electroencephalography (EEG), with its non-invasive and portable

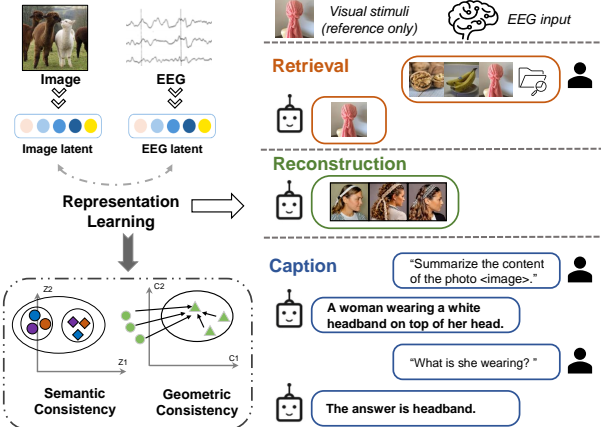


Fig. 1: Conceptual Overview. Left: The RealMind framework employs representation learning to align the semantic and geometric representations of images and EEG data, enforcing constraints on both semantic and geometric consistency. Right: The aligned EEG representations enable a variety of downstream decoding tasks.

nature, offers several distinct advantages over fMRI, including significantly lower acquisition costs and enhanced practicality in real-world applications. Therefore, harnessing multi-modal models for visual decoding from EEG signals constitutes a pivotal advancement, unlocking significant enhancements in both accessibility and scalability for practical applications.

Recently, research on utilizing large multi-modal models

*: Co-first: Dongyang Li and Haoyang Qin.

†: Corresponding to Quanying Liu and Chen Wei.

for visual captioning from EEG data remains limited [17], [18], [22]. This is primarily due to the complex nature of neural data, which is characterized by high dimensionality and inherent noise, making it challenging to develop effective EEG representations for decoding visual information—let alone generating captions based on visual input. However, in the field of fMRI-based visual decoding, several pioneering studies have successfully integrated advanced multi-modal models to decode information from fMRI and reconstruct corresponding images and textual descriptions [4], [12]. For instance, *BrainCaption* [4] combines fMRI with large language model and latent diffusion model to reconstruct images and descriptive caption from brain activity. Similarly, *BrainCLIP* [33] employed contrastive learning techniques to align fMRI signals with both image and text features, enabling efficient cross-modal decoding. Furthermore, *UMBRAE* [11] utilizes a universal brain encoder for multi-modal alignment and implements cross-subject training strategies to address inter-subject variability. These fMRI-based studies serve as inspiration for applying multi-modal models and alignment techniques to the field of EEG decoding.

In this study, we introduce the **RealMind** framework (Fig. 1, left), designed to align EEG representations with pre-trained multi-modal models. RealMind serves as a versatile foundation for improving the performance of various downstream EEG decoding tasks (Fig. 1, right). Our framework demonstrates substantial improvements in both task-specific performance and generalization, while also offering valuable theoretical insights into cross-modal representation learning. Our main contributions are as follows:

- By reinforced representation learning, RealMind is able to adapt various down-stream decoding tasks, including image retrieval, reconstruction and captioning, supporting the practical feasibility of EEG-based visual decoding.
- Our results demonstrate that enforcing semantic and geometric consistency in the latent space promotes better alignment between EEG and image features, achieving a Top-5 accuracy of **56.73%** in a 200-way retrieval task, while also enhancing performance in downstream tasks.
- By leveraging a pre-trained large language model, we successfully achieve zero-shot visual captioning from EEG data for the first time, attaining a BLEU-1 score of **26.59%** in a 200-way captioning task.

II. METHODS

Previous methods [1], [3] often employ contrastive learning and consistency loss to guide the learning process. However, these approaches primarily adjust EEG features based on mean variance and value similarity. In contrast, our approach introduces additional semantic and geometric consistency losses to regulate the representation learning between EEG and image features (Fig. 2). For each sampled batch of EEG and image data pairs, we compute a semantic consistency loss within the semantic space, ensuring coherent alignment of representations across modalities.

The objective of the semantic consistency loss can be summarized as follows:

$$\mathcal{L}_{semantic}(\theta) = \|\mathbf{M}_h^I - \mathbf{M}_h^X\|_F^2 / B^2$$

There, $\mathbf{M}_h^I \in \mathbb{R}^{B \times B}$ represents the cosine similarity matrix of image features extracted from CLIP consisted of the i -th and j -th, $\mathbf{M}_h^X \in \mathbb{R}^{B \times B}$ represents the cosine similarity matrix of EEG features $[i]$ and $[j]$.

Using geometric consistency loss like [34], we adjust the EEG encoder's model parameters to minimize the distance between the EEG feature vector and the image feature vector of the same category, denoted as $d_{min,k}$, as output by the adjusted EEG encoder. Within each class's latent vector, This involves identifying the minimum distance between sample pairs of the same category within the same semantic set and using this template to adjust the distances between other sample pairs. For each batch size data pairs, this ensures that sample pairs within the same category exhibit closer geometric distances $z_{b,i}^s, z_{v,i}^s, y_i^N_{i=1}$, where y_i represents the true label of the sample, $z_{b,i}^s$ represents the i -th EEG feature, and $z_{v,i}^s$ represents the j -th image feature:

$$d_{min,k} = \min\{G(z_{b,i}^s, z_{v,j}^s) \mid y_i = y_j = k, \forall i, j \in \{1, \dots, N\}\}$$

where k is the number of categories, i, j represent the sample numbers for EEG and images respectively, $G(z_b^s, z_v^s) = e^{-t\|z_b^s - z_v^s\|}$ is the Gaussian latent kernel function, and $t = 2$, $d_{min,k}$ represents the minimum distance for a specific category within the batch. Next, we aim for the distance between each modality pair to approximate $d_{min,k}$. The statistical distance loss can be expressed as:

$$\mathcal{L}_{geometric}(\theta) = \sum_{i=0}^N \sum_{j=0}^N I(Y_i, Y_j) (G(z_{b,i}^s, z_{v,j}^s) - d_{min,k}),$$

where $I(Y_i, Y_j) = 1$, if $z_{b,i}^s$ and $z_{v,j}^s$ belong to the same category; $I(Y_i, Y_j) = 0$, otherwise.

The CLIP loss [32] is used on batches of size N with exactly one positive example:

$$\mathcal{L}_{contrastive}(\theta) = \mathcal{L}_{CLIP}.$$

This process is performed using the standard mean squared error (MSE) loss function over the z_i and \hat{z}_i :

$$\mathcal{L}_{MSE}(\theta) = \frac{1}{N} \sum_{i=1}^N \|z_i - \hat{z}_i\|_2^2.$$

The total loss function is composed of several terms, each weighted by a coefficient to control its contribution:

$$\begin{aligned} \mathcal{L}_{total} = & \alpha_1 \mathcal{L}_{mse} + \\ & \alpha_2 \mathcal{L}_{contrastive} + \alpha_3 \mathcal{L}_{semantic} + \alpha_4 \mathcal{L}_{geometric}, \end{aligned}$$

where the coefficients $\alpha_1, \alpha_2, \alpha_3$, and α_4 respectively control the contributions of different loss terms. In the EEG caption task, only \mathcal{L}_{mse} is retained.

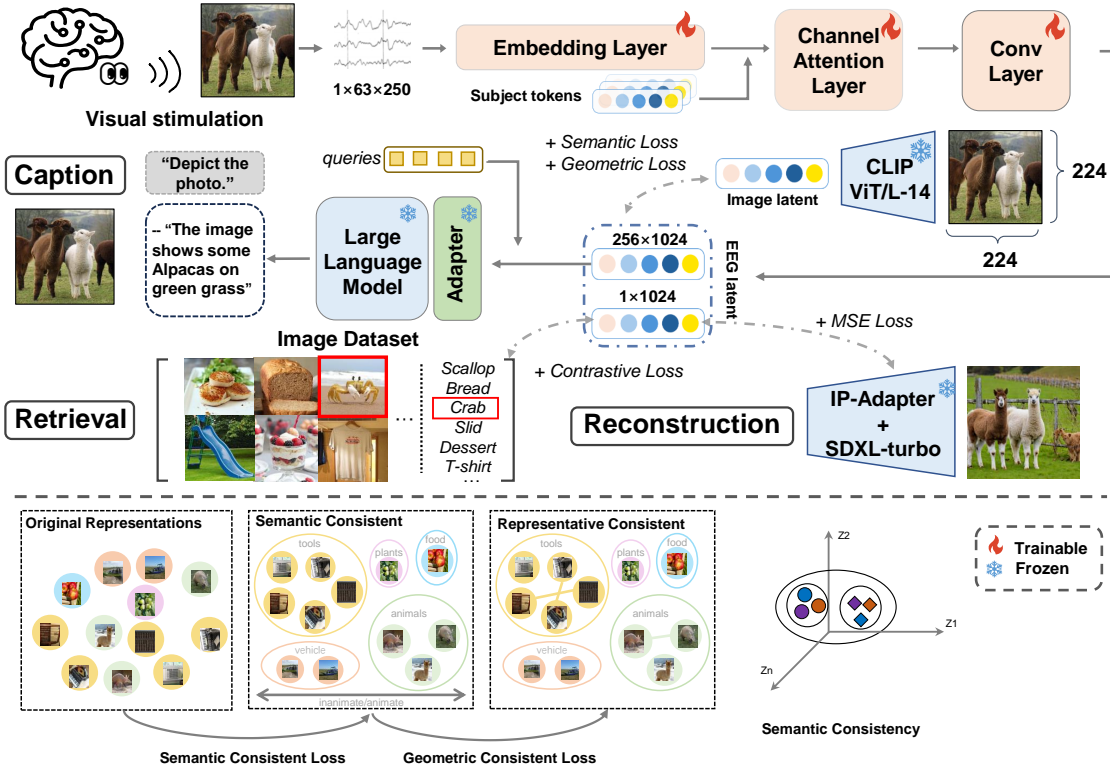


Fig. 2: **RealMind framework.** Top: A Transformer-based model first projects EEG signals to an initial latent space. Convolutional layers and an MLP projector then output CLIP ViT/14-L embeddings. These embeddings are used by SDXL to retrieve and reconstruct the corresponding image. EEG embeddings are subsequently captioned by a pre-trained LLM. Bottom: Semantically similar brain activities exhibit analogous patterns, and similar objects elicit comparable neural responses regardless of labels, highlighting the importance of geometric properties in compressed EEG and image representations within the feature space.

III. EXPERIMENTS AND RESULTS

We conducted comprehensive experiments on THINGS-EEG dataset [14], which is a large-scale, open-access dataset that combines EEG recordings with visual stimuli. All experiments were completed on a single NVIDIA A100 GPU. To train RealMind, We employed the AdamW optimizer to train the in-subject model on a set of EEG 66,160 samples, with an initial learning rate of 3×10^{-4} and batch sizes of 1024. Subject tokens represent the one-hot encoding of each subject, which is used to distinguish the characteristics of each subject. We tested RealMind on the zero-shot test dataset at the end of each training epoch.

We compared the image retrieval performance of various methods from the average all subjects, with the results in Table I. We employed the two-stage reconstruction method proposed by [3] to generate reconstructed images from EEG data in subject-08. Additionally, we obtained captions from the EEG latent representations of subject-08 using a model similar to Llama2 [31].

We equipped RealMind EEG representations with the Shikra model for captioning task (in Fig. 3) and Visual Question and Answering (VQA) task (in Fig. 4). The results show that

TABLE I: Overall accuracy of zero-shot retrieval on THINGS-EEG dataset. We compared the 2-way, 10-way, the Top-1 and Top-5 accuracy of 200-way from different EEG embedding methods.

Dataset	Model	2-way		10-way		200-way	
		Top-1	Top-5	Top-1	Top-5	Top-1	Top-5
THINGS	Benchetrit et al. [1]	91.14	62.62	16.29	42.16		
	Song et al. [6]	92.17	65.65	19.40	46.26		
	Lawhern et al. [2]	89.03	56.77	13.29	35.5		
	Li et al. [3]	93.89	71.63	22.84	52.22		
	Ours	94.34	73.33	24.70	56.73		

RealMind effectively captures and represents the visual stimuli experienced by subjects throughout the experiment. In zero-shot scenarios, our approach outperforms methods that first reconstruct the image and then generate captions. As shown in Table II and Fig. 3, our EEG latent space achieves robust alignment during the representation learning phase, resulting in superior decoding performance across different evaluations.

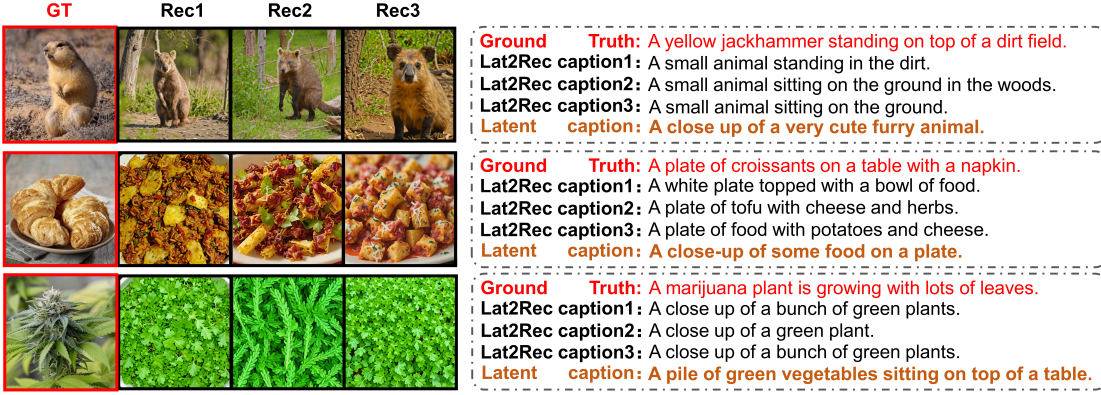


Fig. 3: **Samples of EEG-based image captions generated by RealMind.** Different stages of processing the same input brain signal produce distinct outcomes. We present three examples of images from subject-08. Left: from left to right, the original image followed by three reconstructed images. Right: from top to bottom, the captions for the original image (i.e., ground truth), the three reconstructed images (i.e., Lat2Rec caption), and the EEG latent representation (i.e., Latent caption).

TABLE II: Evaluation of EEG-to-image captions. we used different ground-truth captions for comparison (e.g., Shikra [10] captions, GIT [13] captions or captions generated from BLIP2 [9]). *Abbrev.* L2Cap: directly generating captions from EEG latent; I2Cap: reconstructing images and then generating captions.

Metric	Shikra captions		GIT captions		BLIP2 captions	
	L2Cap	I2Cap	L2Cap	I2Cap	L2Cap	I2Cap
BLEU-1 ↑	26.59	23.09	15.43	18.28	18.31	25.97
BLEU-4 ↑	4.31	3.88	2.90	3.70	3.25	4.65
METEOR ↓	17.79	15.00	15.43	14.20	15.01	18.40
Sentence ↑	17.76	19.62	14.26	23.78	15.60	25.99
CLIP-ViT-L ↑	55.78	53.91	57.83	61.34	58.77	57.52

IV. DISCUSSION AND CONCLUSION

In this paper, we introduced RealMind, a novel framework for EEG-based visual decoding. By integrating semantic and geometric constraints during the representation learning phase, RealMind achieved more efficient alignment with human cognitive processes, significantly enhancing the accuracy and robustness of EEG-based visual semantic decoding. Our model delivered state-of-the-art performance in both retrieval and reconstruction tasks. Additionally, by incorporating a large language model, RealMind successfully generated credible captions from EEG representations. To our knowledge, RealMind is the first framework to achieve zero-shot visual captioning using EEG data.

RealMind advances current EEG visual decoding approaches in two key aspects. First, we introduced a loss function specifically designed for EEG data, significantly improving alignment performance. EEG, compared to fMRI, has long faced challenges such as high noise levels and poor data quality, which have hindered its decoding performance [1]. Our results demonstrate that the additional semantic and geometric loss functions enhanced data utilization efficiency,

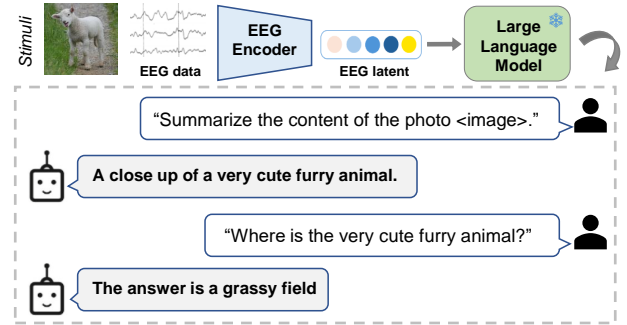


Fig. 4: **Examples of generated answers using RealMind.** Different task prompts for the same input brain signal result in unique outcomes.

leading to improved decoding performance. This is attributed to better feature alignment and the successful integration of large language models. Moreover, we presented the first effective EEG-based captioning solution, paving the way for practical applications in EEG decoding. Compared to fMRI-based visual decoding methods, EEG offers a cost-effective and more accessible alternative. In our previous work [3], we showed that EEG can achieve comparable performance to fMRI in image reconstruction. Here, we further extend EEG-based visual decoding to zero-shot visual captioning tasks.

In the future, we aim to deepen the integration of EEG with multimodal data by incorporating neural data with other data types into a unified multimodal model, rather than simply adding isolated modules. Aligned with the trend of multimodal models, our goal is to develop a single, unified framework capable of handling multiple EEG-based decoding tasks, such as retrieval, reconstruction, and captioning. This approach will enhance data utilization efficiency, enabling limited EEG data to more effectively leverage information from visual and language modalities, ultimately providing a strong foundation for the broader application of EEG-based BCI systems.

REFERENCES

[1] Y. Benchetrit, H. Banville, and J.-R. King, “Brain decoding: toward real-time reconstruction of visual perception,” *arXiv preprint arXiv:2310.19812*, 2023.

[2] V. J. Lawhern, A. J. Solon, N. R. Waytowich, S. M. Gordon, C. P. Hung, and B. J. Lance, “Eegnet: a compact convolutional neural network for eeg-based brain–computer interfaces,” *Journal of neural engineering*, vol. 15, no. 5, p. 056013, 2018.

[3] D. Li, C. Wei, S. Li, J. Zou, and Q. Liu, “Visual decoding and reconstruction via eeg embeddings with guided diffusion,” *arXiv preprint arXiv:2403.07721*, 2024.

[4] M. Ferrante, F. Ozcelik, T. Boccato, R. VanRullen, and N. Toschi, “Brain captioning: Decoding human brain activity into images and text,” *arXiv preprint arXiv:2305.11560*, 2023.

[5] P. S. Scotti, M. Tripathy, C. K. T. Villanueva, R. Kneeland, T. Chen, A. Narang, C. Santhirasegaran, J. Xu, T. Naselaris, K. A. Norman *et al.*, “Mindeye2: Shared-subject models enable fmri-to-image with 1 hour of data,” *arXiv preprint arXiv:2403.11207*, 2024.

[6] Y. Song, B. Liu, X. Li, N. Shi, Y. Wang, and X. Gao, “Decoding natural images from eeg for object recognition,” *arXiv preprint arXiv:2308.13234*, 2023.

[7] W. Mai and Z. Zhang, “Unibrain: Unify image reconstruction and captioning all in one diffusion model from human brain activity,” *arXiv preprint arXiv:2308.07428*, 2023.

[8] Y. Takagi and S. Nishimoto, “High-resolution image reconstruction with latent diffusion models from human brain activity,” in *Proceedings of the IEEE/CVF Conference on Computer Vision and Pattern Recognition*, 2023, pp. 14 453–14 463.

[9] J. Li, D. Li, S. Savarese, and S. Hoi, “Blip-2: Bootstrapping language-image pre-training with frozen image encoders and large language models,” in *International conference on machine learning*. PMLR, 2023, pp. 19 730–19 742.

[10] K. Chen, Z. Zhang, W. Zeng, R. Zhang, F. Zhu, and R. Zhao, “Shikra: Unleashing multimodal llm’s referential dialogue magic,” *arXiv preprint arXiv:2306.15195*, 2023.

[11] W. Xia, R. de Charette, C. Öztïreli, and J.-H. Xue, “Umbrae: Unified multimodal decoding of brain signals,” *arXiv preprint arXiv:2404.07202*, 2024.

[12] G. Shen, D. Zhao, X. He, L. Feng, Y. Dong, J. Wang, Q. Zhang, and Y. Zeng, “Neuro-vision to language: Image reconstruction and interaction via non-invasive brain recordings,” *arXiv preprint arXiv:2404.19438*, 2024.

[13] J. Wang, Z. Yang, X. Hu, L. Li, K. Lin, Z. Gan, Z. Liu, C. Liu, and L. Wang, “Git: A generative image-to-text transformer for vision and language,” *arXiv preprint arXiv:2205.14100*, 2022.

[14] A. T. Gifford, K. Dwivedi, G. Roig, and R. M. Cichy, “A large and rich eeg dataset for modeling human visual object recognition,” *NeuroImage*, vol. 264, p. 119754, 2022.

[15] T. Fang, Q. Zheng, and G. Pan, “Alleviating the semantic gap for generalized fmri-to-image reconstruction,” *Advances in Neural Information Processing Systems*, vol. 36, 2024.

[16] Q. Zhou, C. Du, S. Wang, and H. He, “Clip-mused: Clip-guided multi-subject visual neural information semantic decoding,” *arXiv preprint arXiv:2402.08994*, 2024.

[17] S. Palazzo, C. Spampinato, I. Kavasidis, D. Giordano, J. Schmidt, and M. Shah, “Decoding brain representations by multimodal learning of neural activity and visual features,” *IEEE Transactions on Pattern Analysis and Machine Intelligence*, vol. 43, no. 11, pp. 3833–3849, 2020.

[18] C. Du, K. Fu, J. Li, and H. He, “Decoding visual neural representations by multimodal learning of brain-visual-linguistic features,” *IEEE Transactions on Pattern Analysis and Machine Intelligence*, vol. 45, no. 9, pp. 10 760–10 777, 2023.

[19] F. Ozcelik and R. VanRullen, “Natural scene reconstruction from fmri signals using generative latent diffusion,” *Scientific Reports*, vol. 13, no. 1, p. 15666, 2023.

[20] L. Muttenhaler, L. Linhardt, J. Dippel, R. A. Vandermeulen, K. Hermann, A. Lampinen, and S. Kornblith, “Improving neural network representations using human similarity judgments,” *Advances in Neural Information Processing Systems*, vol. 36, 2024.

[21] J. Li, D. Li, C. Xiong, and S. Hoi, “Blip: Bootstrapping language-image pre-training for unified vision-language understanding and generation,” in *International conference on machine learning*. PMLR, 2022, pp. 12 888–12 900.

[22] F. Yang, C. Feng, D. Wang, T. Wang, Z. Zeng, Z. Xu, H. Park, P. Ji, H. Zhao, Y. Li *et al.*, “Neurobind: Towards unified multimodal representations for neural signals,” *arXiv preprint arXiv:2407.14020*, 2024.

[23] J. Han, K. Gong, Y. Zhang, J. Wang, K. Zhang, D. Lin, Y. Qiao, P. Gao, and X. Yue, “Onellm: One framework to align all modalities with language,” in *Proceedings of the IEEE/CVF Conference on Computer Vision and Pattern Recognition*, 2024, pp. 26 584–26 595.

[24] Z. Lin, C. Liu, R. Zhang, P. Gao, L. Qiu, H. Xiao, H. Qiu, C. Lin, W. Shao, K. Chen *et al.*, “Sphinx: The joint mixing of weights, tasks, and visual embeddings for multi-modal large language models,” *arXiv preprint arXiv:2311.07575*, 2023.

[25] H. Liu, C. Li, Q. Wu, and Y. J. Lee, “Visual instruction tuning,” *Advances in neural information processing systems*, vol. 36, 2024.

[26] Y. Zhang, K. Gong, K. Zhang, H. Li, Y. Qiao, W. Ouyang, and X. Yue, “Meta-transformer: A unified framework for multimodal learning,” *arXiv preprint arXiv:2307.10802*, 2023.

[27] J. Han, R. Zhang, W. Shao, P. Gao, P. Xu, H. Xiao, K. Zhang, C. Liu, S. Wen, Z. Guo *et al.*, “Imagebind-llm: Multi-modality instruction tuning,” *arXiv preprint arXiv:2309.03905*, 2023.

[28] C. Wei, J. Zou, D. Heinke, and Q. Liu, “Cocog: Controllable visual stimuli generation based on human concept representations,” *arXiv preprint arXiv:2404.16482*, 2024.

[29] ———, “Cocog-2: Controllable generation of visual stimuli for understanding human concept representation,” *arXiv preprint arXiv:2407.14949*, 2024.

[30] H. Touvron, T. Lavril, G. Izacard, X. Martinet, M.-A. Lachaux, T. Lacroix, B. Rozière, N. Goyal, E. Hambro, F. Azhar *et al.*, “Llama: Open and efficient foundation language models,” *arXiv preprint arXiv:2302.13971*, 2023.

[31] H. Touvron, L. Martin, K. Stone, P. Albert, A. Almahairi, Y. Babaei, N. Bashlykov, S. Batra, P. Bhargava, S. Bhosale *et al.*, “Llama 2: Open foundation and fine-tuned chat models,” *arXiv preprint arXiv:2307.09288*, 2023.

[32] A. Radford, J. W. Kim, C. Hallacy, A. Ramesh, G. Goh, S. Agarwal, G. Sastry, A. Askell, P. Mishkin, J. Clark *et al.*, “Learning transferable visual models from natural language supervision,” in *International conference on machine learning*. PMLR, 2021, pp. 8748–8763.

[33] Y. Liu, Y. Ma, W. Zhou, G. Zhu, and N. Zheng, “Brainclip: Bridging brain and visual-linguistic representation via clip for generic natural visual stimulus decoding,” *arXiv preprint arXiv:2302.12971*, 2023.

[34] H. Chen, L. He, Y. Liu, and L. Yang, “Visual neural decoding via improved visual-eeg semantic consistency,” *arXiv preprint arXiv:2408.06788*, 2024.

[35] P. Scotti, A. Banerjee, J. Goode, S. Shabalin, A. Nguyen, A. Dempster, N. Verlinde, E. Yundler, D. Weisberg, K. Norman *et al.*, “Reconstructing the mind’s eye: fmri-to-image with contrastive learning and diffusion priors,” *Advances in Neural Information Processing Systems*, vol. 36, 2024.